Line Position and Quality Factor of Plasmonic Resonances Beyond the Quasi-Static Limit: A Full-Wave Eigenmode Analysis Route

Xuezhi Zheng, Vladimir Volskiy, *Member, IEEE*, Ventsislav K. Valev, Guy A. E. Vandenbosch, *Senior Member, IEEE*, and Victor V. Moshchalkov

***Abstract*—In this study, we introduce a rigorous full-wave eigenmode analysis technique based on a volumetric method of moments to the optical spectrum. We first apply this technique to a nanorod as an example to illustrate how the real part of the eigenfrequency and the modal quality factor (defined as the ratio of the real part of the eigenfrequency to the imaginary part) together with the eigenmode determine the line position and quality factor of a resonance and the corresponding resonant mode. Then, the eigenfrequencies and eigenmodes of a composite plasmonic nanostructure, a Dolmen, and its two individual constituents, a dimer and a monomer, are extracted. The line position of the Fano dip in Dolmen's spectrum is discussed by examining the relative positions of the eigenfrequencies of the dimer and the monomer in the complex plane. Further, the formation of the Fano dip is reinterpreted as the destructive interference between the nonorthogonal eigenmodes of the whole Dolmen structure. The proposed full-wave modal analysis brings a new perspective on understanding and designing the plasmonic response of nanoantennae beyond the quasi-static limit.**

***Index Terms*—Eigenmode analysis, nanoantennae, plasmonics, volumetric method of moments (V-MoM).**

I. Introduction

THE antenna as an object converting radiative energy into localized energy and vice versa [1] has found wide applications at both microwave and optical frequencies. At optical frequencies, due to its possible subwavelength scale, nanoantennae can be exploited as a powerful tool to overcome the diffraction limit. Many topologies, like the monopole [2], dipole [3], Yagi-Uda [4], etc., have been studied at optical frequencies. Several attempts have been made in order to bridge the gap between microwave and optical frequencies and to migrate the state of the art in antenna design from microwave to optical frequencies. For example, in order to generalize the microwave antenna linear scaling rule to optical frequencies, Novotny [5] exploits a relation that converts the vacuum wavelength to an effective wavelength. Another example can be found in the "lumped circuit" model, which was reintroduced by Engheta *et al*. [6] in the optical regime in parallel with the tradition at microwaves. Moreover, De Arquer *et al*. [7] analyze the nanodipole antenna by means of its input impedance as well as the matching properties of the antenna topology and material configuration. All of these approaches are based on design rules and circuit models. As such, they provide a practical guideline for transferring microwave know-how to the optical spectrum.

Alternatively, in the course of understanding electromagnetic wave propagation and electromagnetic scattering problems, eigenmode analysis can be employed, because this method isolates the system under study from the excitation, and thus gives the most intrinsic description of the problem. Several problems, e.g., the propagation of electromagnetic waves in rectangular and cylindrical waveguides or the scattering of electromagnetic waves by metallic spheres, have been solved analytically and the solution can be found in classic textbooks [8], [9]. Moreover, eigenmode analysis has found wide application at microwave frequencies, e.g., in the study of the interaction of an electromagnetic pulse (EMP) with metallic objects at microwave frequencies, coined by Baum [10] as the singularity expansion method, and in the calculation of radar scattering patterns [11].

Inspired by the spirit of modal analysis, within the quasi-static limit, at optical frequencies, several research groups apply eigenmode analysis to isolated [12], [13] and coupled [14]–[16] nanoparticles. Similarly, based on the zeroth order Bergman–Milton spectral representation [17]–[19], the effective permittivity of a nanostructured material can be designed [20]. Its value is limited by Bergman–Milton bounds [21]. Since in these cases the wavelength of the incident electromagnetic wave is assumed to be much larger than the size of the nanoparticles, the dynamic aspects, including retardation and dissipation, are neglected. Consequently, the eigenfrequencies of the systems under consideration always lie on the real frequency axis.

Yet, for nanostructures beyond the quasi-static limit, it is well known that the optical loss, including radiative [22] and ohmic [23], [24] loss, strongly affects the spectral position and

Manuscript received June 30, 2012; revised September 7, 2012; accepted October 22, 2012. Date of publication November 15, 2012; date of current version April 25, 2013. This work was supported by the Fund for Scientific Research Flanders, Katholieke Universiteit Leuven (GOA), and the Flemish Government through Methusalem Funding. The work of V. K. Valev was supported by the FWO-Vlaanderen, Consorcios Regionales de Experimentación Agricola, and the Engineering and Physical Sciences Research Council under Grant EP/G060649/1.

X. Zheng, V. Volskiy, and G. A. E. Vandenbosch are with the Department of Electrical Engineering, Katholieke Universiteit Leuven, 3001 Leuven, Belgium (e-mail: xuezhi.zheng@esat.kuleuven.be; vladimir.volski@esat.kuleuven.be; guy.vandenbosch@esat.kuleuven.be).

V. K. Valev is with Cavendish Laboratory, Department of Physics, University of Cambridge, Cambridge, CB3 0HE, U.K. (e-mail: ventsislav.valev@fys.kuleuven.be).

V. V. Moshchalkov is with the Nanoscale Superconductivity and Magnetism, Pulsed Fields Group, Department of Physics, Katholieke Universiteit Leuven, 3001 Leuven, Belgium (e-mail: Victor.Moshchalkov@fys.kuleuven.be).

Color versions of one or more of the figures in this paper are available online at http://ieeexplore.ieee.org.

Digital Object Identifier 10.1109/JSTQE.2012.2227684

broadens the linewidth of the plasmonic resonances. In order to fully characterize the effects of these decay channels, an extra axis, i.e., the imaginary axis, must be exploited and the eigenmode analysis must be performed in the 2-D complex plane.

The purpose of this study is threefold. 1) In order to perform a full-wave modal analysis to nanostructures with increasing complexity, the interaction of light with nanostructures is formulated as an eigenvalue problem which is, to the knowledge of the authors, solved by a volumetric method of moments (V-MoM) algorithm for the first time. 2) The relations between the complex eigenfrequencies and two design parameters of great interest, namely the line position and the quality factor [25], [26] of surface plasmon resonances are exploited. It is shown that the real part of an eigenfrequency determines the spectral position of the plasmonic resonance. A modal quality factor Q_{mod}, defined as the ratio of the real part of the eigenfrequency to the imaginary part of the eigenfrequency, characterizes the "life time" of the plasmonic mode. The quality factor of resonance Q_{res} can be estimated from Q_{mod} by looking at the contributions of different eigenmodes. 3) The eigenfrequencies and eigenmodes of a composite nanostructure, a Dolmen, are calculated. The physical origin of the Fano dip in its spectrum is discussed by looking at the positions of the eigenfrequencies of its individual constituents, the dimer and the monomer, in the complex plane. Further, a new physical interpretation is given to a Fano dip: it is considered as the result of the destructive interference between two nonorthogonal eigenmodes of the whole Dolmen structure.

II. Light–Plasmonic Nanoparticle Interaction Formulated as an Eigenvalue Problem

In order to formulate the interaction of light with nanoplasmonic antennae as an eigenvalue problem, consider a nanometallic scatterer excited by incident light. As a consequence of the excitation, a polarization current $\mathbf{J}(\mathbf{r}')$ flows on the scatterer obeying the following set of equations:

$$\mathbf{E}^{\mathbf{tot}}(\mathbf{r}) = \mathbf{E}^{\mathbf{inc}}(\mathbf{r}) + \mathbf{E}^{\mathbf{sca}}(\mathbf{r}) \tag{1}$$

$$\mathbf{E}^{\mathbf{sca}}(\mathbf{r}) = -i\omega\mu_0 \int_V \mathbf{G}(\mathbf{r},\mathbf{r}',\omega)\cdot\mathbf{J}(\mathbf{r}')\,dV' \tag{2}$$

$$\mathbf{E}^{\mathbf{tot}}(\mathbf{r}) = \frac{\mathbf{J}(\mathbf{r})}{i\omega\left(\varepsilon_v(\omega,\mathbf{r}) - \varepsilon_k\right)}. \tag{3}$$

Notice that the time convention $e^{i\omega t}$ is employed. Equation (1) states that the total electric field $\mathbf{E}^{\mathbf{tot}}(\mathbf{r})$ is the sum of the incident field $\mathbf{E}^{\mathbf{inc}}(\mathbf{r})$ and the scattered field $\mathbf{E}^{\mathbf{sca}}(\mathbf{r})$. Equation (2) states that this scattered field actually originates from the polarization current $\mathbf{J}(\mathbf{r})$ induced on the scatterer. It is a 3-D convolution of this current and a tensor Green's function $\mathbf{G}(\mathbf{r},\mathbf{r}',\omega)$. Equation (3) expresses the relation between the total electric field present at a location within the scatterer and the complex and possibly dispersive permittivity $\varepsilon_\nu(\omega,\mathbf{r}')$ of the material there. ε_k is the permittivity of the surrounding environment. Note that for nanostructures operating at optical frequencies, the skin depth may be comparable with the structural dimensions, so that currents do flow over the complete volume and the integration must be performed with respect to that volume. A surface current description is not sufficient. Combining the three equations yields an equation for the current

$$i\omega\mu_0 \int_{V'} \mathbf{G}(\mathbf{r},\mathbf{r}',\omega)\cdot\mathbf{J}(\mathbf{r}')\,dV' + \frac{\mathbf{J}(\mathbf{r})}{i\omega\left(\varepsilon_\nu(\omega,\mathbf{r}) - \varepsilon_k\right)} = \mathbf{E}^{\mathbf{inc}}(\mathbf{r}). \tag{4}$$

Equation (4) is traditionally solved numerically. A classical technique is to use the method of moments [27]. First, the nanostructure is discretized and the current is approximated by n discrete basis functions

$$\mathbf{J} = \sum_{i=1}^{n} I_i \mathbf{f}_i. \tag{5}$$

Then, n test functions are applied to evaluate in an average sense. This leads to a matrix formulation of the problem

$$\mathbf{Z}(\omega)\,\mathbf{I}(\omega) = \mathbf{E}^{\mathbf{inc}}(\omega) \tag{6}$$

where $\mathbf{Z}$ is an $n \times n$ matrix, and $\mathbf{I}$ and $\mathbf{E}^{\mathbf{inc}}$ are $n \times 1$ column vectors.

An eigenfrequency ω_m of the scatterer is by definition a frequency at which a nonzero solution for the current can be found for a zero excitation. In other words

$$i\omega_m\mu_0 \int_{V'} \mathbf{G}(\mathbf{r},\mathbf{r}',\omega_m)\cdot\mathbf{J}_m(\mathbf{r}')dV' + \frac{\mathbf{J}_m(\mathbf{r})}{i\omega_m\left(\varepsilon_\nu(\omega_m,\mathbf{r}) - \varepsilon_k\right)} = \mathbf{0} \tag{7}$$

with $\mathbf{J}_m(\mathbf{r}')$ the mth eigenmode current. In the matrix domain, this becomes

$$\mathbf{Z}(\omega)\,\mathbf{I}_m(\omega) = 0. \tag{8}$$

In order to find a nontrivial solution for $\mathbf{I}_m(\omega)$, the determinant of the coupling matrix has to be zero; thus

$$\det(\mathbf{Z}(\omega_m)) = 0. \tag{9}$$

Equation (9) gives the eigenfrequencies in the complex plane of the topology under consideration. The corresponding eigenmode is found by solving (8) at this eigenfrequency. Since this system has now one degree of freedom, due to the fact that the determinant is zero, an additional equation can be imposed. This can be done by requiring the solution to be normalized, i.e., with prescribed current profile amplitude.

III. Line Position and Quality Factor of Surface Plasmon Resonances

According to the previously discussed procedure, the eigenfrequencies and eigenmodes of gold nanorods with different lengths are numerically calculated with the in-house developed MoM code MAGMAS [28]–[31]. The dimensions, materials, mesh sizes, and surroundings of the nanorods are tabulated in Table I. The calculated eigenfrequencies are shown in Fig. 1(a) and tabulated in Table II. The calculated eigenmodes of the 300-nm nanorod are shown in the inset of Fig. 1(a). For clarity, the factor 2π is dropped from all the real parts of the eigenfrequencies.

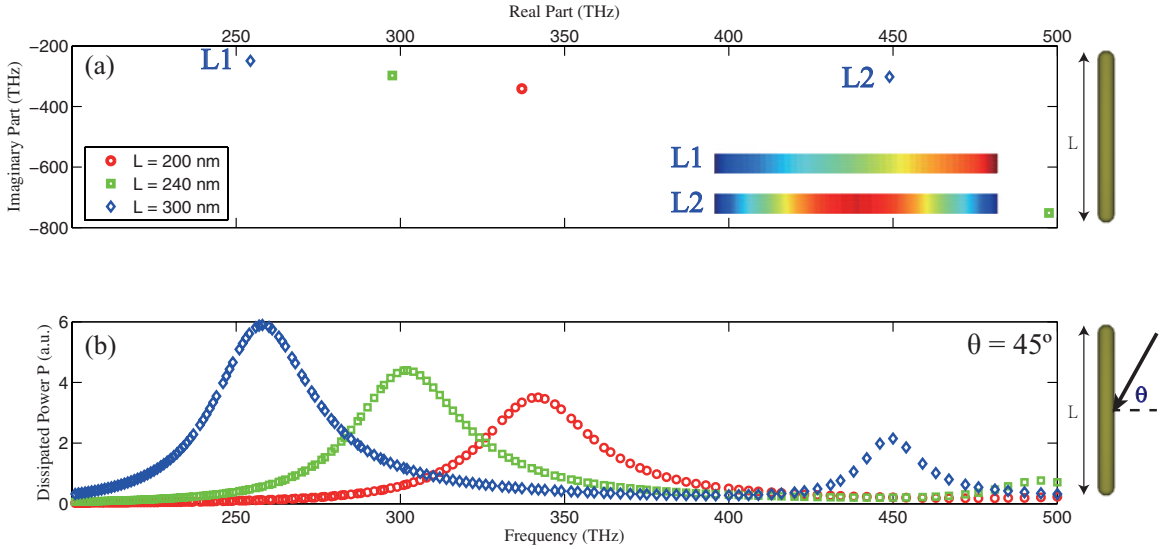

Fig. 1. Complex eigenfrequencies of nanorods determine the line positions of surface plasmon resonances. (a) Complex eigenfrequencies of nanorods of different lengths; the top view of surface charge eigenmodes of the 300-nm nanorod is shown in the inset. (b) Dissipated power for incidence angle 45°; the polarization of the electric field is perpendicular to the direction of propagation and lies in the incidence plane.

TABLE I
PARAMETERS USED IN THE SIMULATIONS

Parameters	Nanorods		
Length (L)	200 nm	240 nm	300 nm
Width (W)	40 nm	40 nm	40 nm
Thickness (T)		40 nm	
Material		Au [32]	
Surrounding		Vacuum	
Mesh cell sizes		20 nm x 20 nm x 20 nm	

TABLE II
EIGENFREQUENCIES OF 200, 240, AND 300-nm NANORODS

Length	Anti-symmetric mode (THz)	Symmetric mode (THz)
200 nm	336.990 - 341.224i	556.564 - 2830.428i
240 nm	297.565 – 297.780i	497.472 – 751.535i
300 nm	254.355 – 249.281	448.910 – 302.259i

A. Line Position of Surface Plasmon Resonance

When an external excitation of frequency ω is applied, the polarization current is solved as from (6)

$$\mathbf{I}(\omega) = \mathbf{Z}^{-1}(\omega) \cdot \mathbf{E}^{\mathbf{inc}}(\omega) = \frac{\mathbf{Y}(\omega)}{\Delta} \cdot \mathbf{E}^{\mathbf{inc}}(\omega). \tag{10}$$

$\mathbf{Y}(\boldsymbol{\omega})$ is the adjoint matrix of the impedance matrix. Δ is the determinant of the impedance matrix, which is a polynomial that can be decomposed into factors $(\omega - \omega_m)^n$. $\omega_m = \omega_{mr} - i\omega_{mi}$ is a calculated eigenfrequency according to (9) and n is the order of the eigenfrequency, indicating the degree of degeneracy of the eigenmodes. For nanorods, only simple poles $(n = 1)$ are present, and the response can be rewritten as

$$\begin{aligned}\mathbf{I}(\omega) &= \sum_m \frac{\mathbf{R}_m}{(\omega - \omega_m)} \cdot \mathbf{E}^{\mathbf{inc}}(\omega) \\ &= \sum_m \frac{\mathbf{j}_m \mathbf{j}_m^T}{(\omega - \omega_m)} \cdot \mathbf{E}^{\mathbf{inc}}(\omega) \\ &= \sum_m \frac{\mathbf{j}_m^T \cdot \mathbf{E}^{\mathbf{inc}}(\omega)}{(\omega - \omega_m)} \mathbf{j}_m \end{aligned} \tag{11}$$

where $\mathbf{R}_m$ is the system residue matrix at each eigenfrequency. It has been shown that $\mathbf{R}_m$ is a dyadic and can be decomposed as the outer product of eigenmode $\mathbf{j}_m$ and its transpose $\mathbf{j}_m^T$ [33]. For monochromatic light of frequency ω around ω_{mr}, the amplitude of $\mathbf{I}(\omega)$ is

$$|\mathbf{I}(\omega)| \propto \frac{1}{\sqrt{(\omega - \omega_{mr})^2 + \omega_{mi}^2}}. \tag{12}$$

It is readily seen from (12) that when ω is around ω_{mr}, the response reaches a maximum. Therefore, the positions of surface plasmon resonances can be correctly predicted by the real parts of the eigenfrequencies, as shown by the line positions of the resonances in Fig. 1(b).

B. Quality Factor Q_{res} of Surface Plasmon Resonances

Furthermore, a modal quality factor Q_{mod} can be defined for each eigenmode. Consider an incoming EMP $\delta(t)$, which contains all frequency components with the same amplitude 1. Equation (11) leads to

$$\mathbf{I}(t) = \sum_m K_m \mathbf{j_m} e^{i\omega_m t}. \tag{13}$$

K_m is defined as the coupling coefficient of the mth surface plasmon eigenmode, which is a constant independent of frequency. In (13), all eigenmodes are present. By noticing that $i\omega_m = -\omega_{mi} + i\omega_{mr}$, each eigenmode oscillates with frequency ω_{mr} but decays with a rate defined by $-\omega_{mi}$. Therefore, the energy decaying rate is

$$-2\omega_{mi} = \frac{P_{\mathrm{dissipated}}}{W_{\mathrm{stored}}}. \tag{14}$$

Based on (14), the "life time" of a surface plasmon eigenmode can be defined as $1/-2\omega_{mi}$. The quality factor Q_{mod} for each

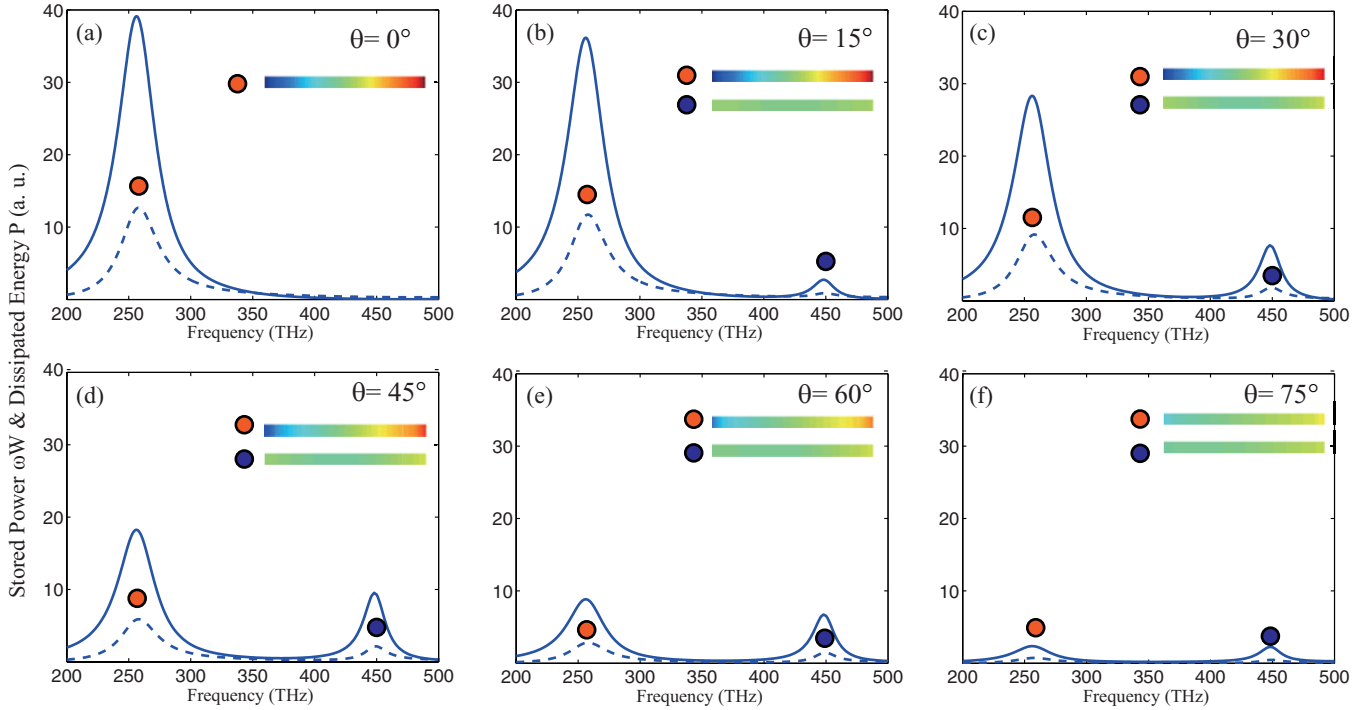

Fig. 2. Stored power (solid line) and dissipated power (dashed line) of the 300-nm nanorod when the nanorod is excited by incident light with different incidence angles. The incident angle and the polarization of the incoming electromagnetic wave are the same as in Fig. 1. The surface plasmon modes at resonance are shown in the insets.

TABLE III
RESONANT FREQUENCY $f_{\rm res}$, STORED POWER ωW, DISSIPATED POWER P, $Q_{\rm res}$ FACTOR AT RESONANCES FOR DIFFERENT INCIDENT ANGLE θ, AND MODAL $Q_{\rm mod}$ FACTOR OF THE 300-nm NANOROD

θ	f_{res}	$\omega W\,(10^{-16})$	$P\,(10^{-16})$	Q_{res}	$Q_{\rm mod}$
0°	255.8 THz (anti-symmetric mode)	39.09	12.47	3.1336	3.2055
15°		36.13	11.53	3.1336	
30°		28.33	9.053	3.1293	
45°		18.25	5.820	3.1357	
60°		8.843	2.841	3.1126	
75°		2.368	0.7338	3.2270	
15°	450THz (symmetric mode)	2.702	0.8788	3.0746	4.6166
30°		7.474	1.849	4.0422	
45°		9.290	2.151	4.3189	
60°		6.555	1.473	4.4501	
75°		2.208	0.4725	4.6730	

eigenmode can be defined as

$$Q_{\rm mod} = \frac{\omega W_{\rm stored}}{P_{\rm dissipated}} = \frac{\omega_{mr}}{-2\omega_{mi}}. \tag{15}$$

When monochromatic light of frequency ω around ω_{mr} is applied, according to (11), assuming that the mth eigenmode is dominant, the response $\mathbf{I}(\omega)$ is

$$\mathbf{I}(\omega) \approx K_m \mathbf{j}_m. \tag{16}$$

By noticing that $K_m = \left(\mathbf{j}_m^T \cdot \mathbf{E}^{\rm inc}(\omega)\right)/(\omega - \omega_m)$ is a scalar, the response $\mathbf{I}(\omega)$ near the resonance is almost determined by the excited eigenmode $\mathbf{j}_m$. Since a fixed distribution of stored energy W and dissipated power P is associated with each eigenmode $\mathbf{j}_m$ oscillating at ω_{mr}, the modal quality factor $Q_{\rm mod}$ should render a good estimation of the quality factor $Q_{\rm res}$ at resonance.

As an illustration, the stored power ωW, the dissipated power P, and the quality factor at resonance (defined as the ratio of the stored power ωW to the dissipated power P at the resonant frequency $\omega_{\rm res}$), when the nanorod of 300 nm is excited by an incident electromagnetic wave with different incidence angles, are calculated from the polarization current flowing inside the structure and plotted in Fig. 2. The details of the calculation can be found in [34]. The quality factor $Q_{\rm res}$ at the resonances and the modal quality factor $Q_{\rm mod}$ are tabulated in Table III. It can be clearly seen that for the antisymmetric mode, a good indication of $Q_{\rm res}$ is given by $Q_{\rm mod}$.

TABLE IV
MONOMER, DIMER, DOLMEN: THE REAL PART OF THE EIGENFREQUENCY, THE MODAL QUALITY FACTOR, THE STORED POWER AT RESONANCE $(\omega \mathrm{W})_{\mathrm{res}}$, THE DISSIPATED POWER P_{res}, AND THE QUALITY FACTOR Q_{res} AT RESONANCE

Structure	f_{real} (THz)	Q_{mod}	f_{res} (THz)	$(\omega W)_{res}$	P_{res}	Q_{res}
Monomer |B>	337	3.1026	338.5	2.201e-15	7.245e-16	3.0380
Dimer |D>	324	8.0258	324.4	2.671e-17	2.173e-18	12.292
Dolmen |B> - |D>	292	5.4104	291.5	2.645e-15	4.931e-16	5.3640
Dolmen |B> + |D>	356	3.6825	357.3	2.071e-15	5.779e-16	3.5837

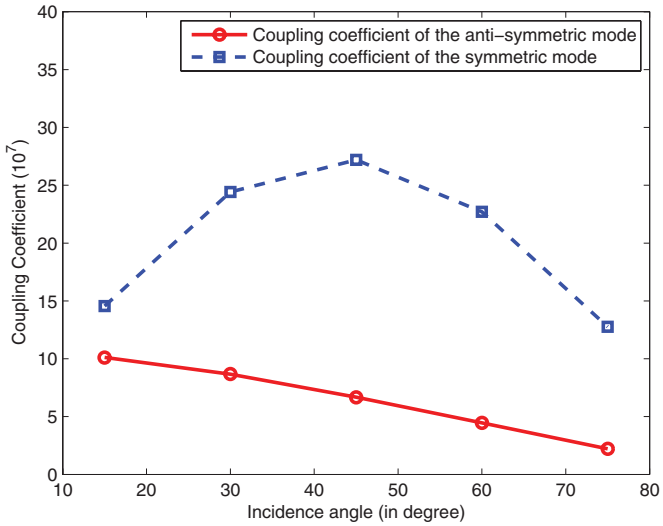

Fig. 3. Coupling coefficient of the antisymmetric mode and coupling coefficient of the symmetric mode of the 300-nm nanorod.

On the other hand, several eigenmodes can contribute to the formation of one single resonant plasmon mode. In order to illustrate this, the response $\mathbf{I}(\omega)$ at the second resonance (450 THz) is calculated by directly solving (6). Then, the coupling coefficients $K_m = \mathbf{j}_m \cdot \mathbf{I}(\omega)$ for the antisymmetric mode $\mathbf{j}_1$ and symmetric mode $\mathbf{j}_2$ are calculated for different incident angles ($\theta = 15^\circ, 30^\circ, 45^\circ, 60^\circ, 75^\circ$) and shown in Fig. 3. Clearly, not one eigenmode only contributes to the second resonance. When the incident angle is 15°, the contributions from the antisymmetric mode and the symmetric mode are comparable, and neither the antisymmetric mode nor the symmetric mode determines Q_{res}, leading to the large deviation from the modal quality factor. As the incidence angle increases, as shown in Fig. 3, the coupling coefficient of the antisymmetric eigenmode K_1 decreases. The symmetric eigenmode plays a dominant role in the response, resulting in the fact that the quality factor Q_{res} approaches the value of the modal quality factor Q_{mod} of the symmetric eigenmode, as shown in Table III.

IV. FULL-WAVE MODAL ANALYSIS OF DOLMEN STRUCTURE

Having clarified the relation between a complex eigenfrequency and the corresponding line position and quality factor of a plasmonic resonance, in this section, we apply the proposed full-wave modal analysis to a composite nanoplasmonic system, a Dolmen structure [35], [36]. The Dolmen structure is of great interest in plasmonic research due to its capability of supporting a Fano resonance, known as a sharp asymmetric line shape. This promises applications in nanoscale sensing and the nanoscale analogy of electromagnetically induced transparency (EIT) [37].

The first two eigenfrequencies and eigenmodes of the Dolmen nanostructure, made of three 200 nm $\times$ 40 nm $\times$ 40 nm gold nanorods, are extracted and plotted in Fig. 4(a) and (c). The gap size between the dimer and the monomer, and the separation distance between the two nanobars in the Dimer are 50 and 20 nm, respectively. The whole Dolmen structure is immersed in vacuum and described with 20 nm $\times$ 20 nm $\times$ 20 nm cells in the numerical study. Again, it can be readily seen from Fig. 4(a) and (b) that the real part of the eigenfrequencies of the Dolmen structure well predicts the line positions of the resonances. Also, it is tabulated in Table IV that the quality factor of the resonances is determined by the corresponding modal quality factor.

Furthermore, it is interesting to study the physical origin of the line position of the Fano dip in Fig. 4(b) by applying the full-wave modal analysis technique. The eigenfrequency of the fundamental eigenmode of the individual monomer and the dimer is extracted. For the monomer, the first eigenmode is a "superradiant" dipolar mode. Its nonzero dipolar moment radiates into free space, contributing to the main channel for the decay of the stored energy. Therefore, the correspondent eigenfrequency has a large imaginary part (a short life time and thus a low modal quality factor). As opposed to the monomer, the first eigenmode of an individual dimer is an electric quadruple mode whose electric dipolar moment is almost zero, thus only weakly coupled to free space, resulting in a slow decaying and a high modal quality factor. Due to the near degeneracy of these two eigenmodes, when properly excited, the Dolmen structure can be coupled with the incident wave $|I\rangle$ via two channels $|I\rangle \rightarrow |B\rangle$ [38], which provides a broad background continuum as implied by the low modal quality factor, and $|I\rangle \rightarrow |B\rangle \rightarrow |D\rangle \rightarrow |B\rangle$, where the "bright" mode mediates free space with the high modal quality factor sharp "dark" dimer. The destructive interference between these two channels leads to the Fano dip in the dissipated energy. At the Fano dip, the Dolmen structure reacts little to the external electromagnetic perturbation, mimicking EIT at nanoscale.

On the other hand, besides the analysis starting from the interaction between the eigenmodes of the constituent nanocavities, the Fano dip can also be understood by closely examining the interaction of the eigenmode $|B\rangle + |D\rangle$ with the eigenmode $|B\rangle - |D\rangle$ of the *whole* Dolmen structure. First of all, the nonorthogonality of these two modes can be readily read from the surface charge distribution, as shown in Fig. 4(c). This is further proved by numerically calculating the inner product of the two modes. Such a nonorthogonality implies that the

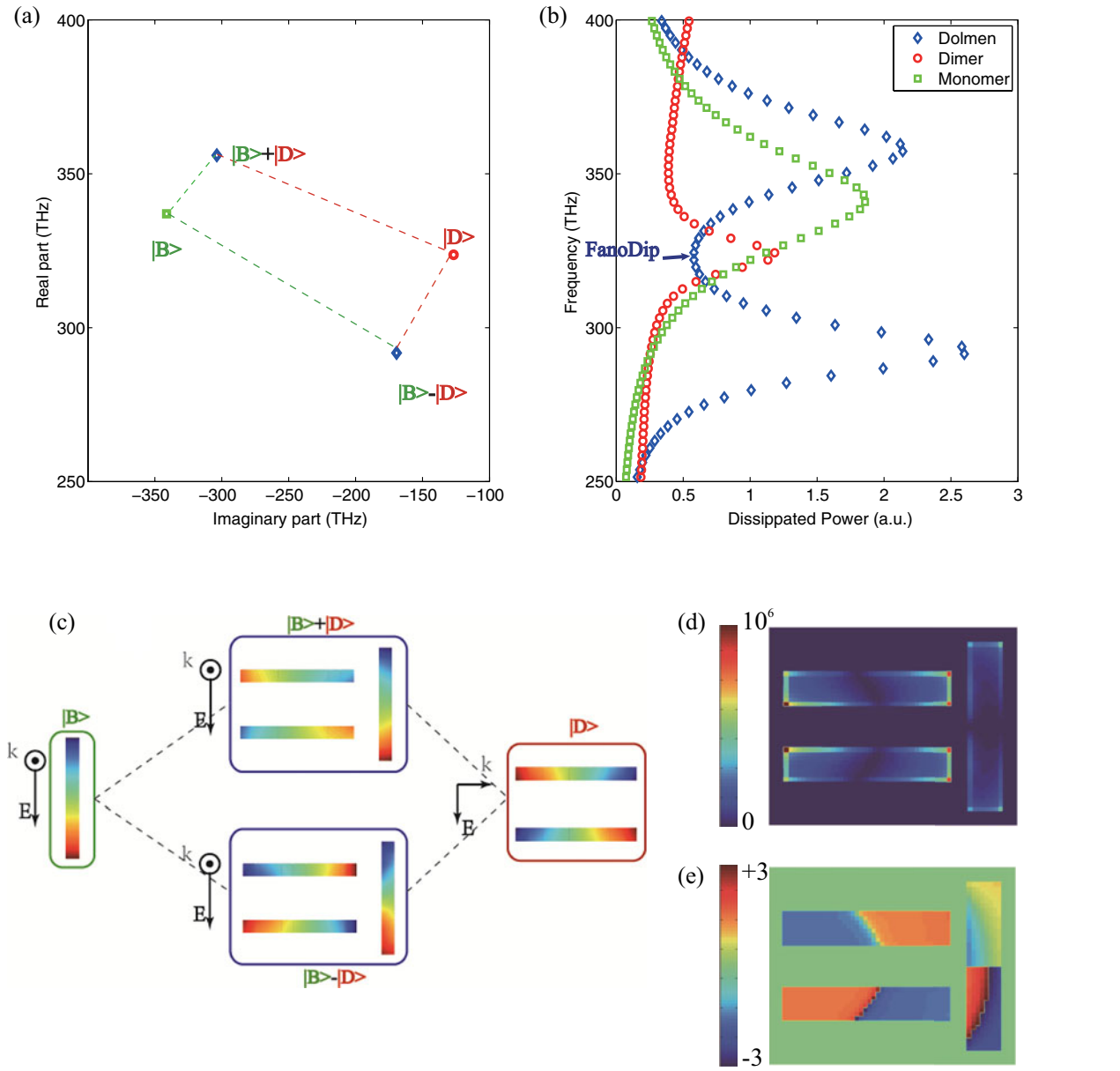

Fig. 4. (a) Hybridization diagram in the complex plane. (b) Dissipated energy of the excited monomer, dimer, and Dolmen structures. (c) Fundamental eigenmode of the monomer and dimer; the first two modes of the Dolmen and the propagation direction and the polarization of the incident electromagnetic field exciting these eigenmodes: |B> is the bright mode for the monomer; |D> is the dark mode for the dimer; |B> − |D> and |B> + |D> are the bonding and antibonding mode for the Dolmen, respectively. (d) and (e) Amplitude and phase of the surface charge at the Fano dip.

excitation of one mode provides a possibility for the other mode to couple with the incident electromagnetic field. At the Fano dip, although the $|B\rangle - |D\rangle$ eigenmode still realizes the major contribution, via the near field coupling, the $|B\rangle + |D\rangle$ eigenmode is excited with the same amplitude but with a $\pi-$phase difference. Therefore, a nonactive monomer and a nonradiating dimer, as shown in Fig. 4(d) and (e), minimize the radiative loss, which results in a dip in the dissipated power spectrum.

V. Conclusion

In summary, the electromagnetic scattering of nanoplasmonic structures beyond the quasi-static limit is formulated as an eigenvalue problem. The eigenfrequencies and eigenmodes are calculated by the V-MoM algorithm. Due to the radiative and ohmic loss of plasmonic nanostructures, the eigenfrequencies are considered in the complex plane. It is shown that the real parts of the eigenfrequencies give the accurate line positions of the resonances, with the eigenmodes defining the resonant modes of the plasmonic responses. Moreover, the imaginary parts of the eigenfrequencies define the energy decaying rate of stored energy via radiative and ohmic loss of the eigenmodes. The modal quality factor Q_{mod} is defined for each eigenmode. With the knowledge of coupling coefficients, the quality factor Q_{res} of the correspondent resonance can be estimated from the modal quality factor Q_{mod}. Further, this method is applied to a

composite nanoplasmonic system to reveal the physical origin of the Fano resonance. The line position of the Fano dip can be pointed out as soon as the eigenfrequencies of the individual constituents are calculated. The formation of the Fano dip is explained from the whole structure point of view. Since the proposed modal analysis does not depend on the excitation, it reveals the most intrinsic aspects of light–metallic nanoparticle interaction and helps designers to thoroughly understand and, thus, tailor the plasmonic response of nanostructures.

REFERENCES

[1] P. Bharadwaj, B. Deutsch, and L. Novotny, "Optical antenna," *Adv. Opt. Photon*., vol. 1, pp. 438–483, 2009.

[2] T. H. Taminiau, F. B. Segerink, R. J. Moerland, L. Kuipers, and N. F. Van Hulst, "Near-field driving of a optical monopole antenna," *J. Opt. A: Pure Appl. Opt*., vol. 9, pp. S315–S321, 2007.

[3] P. Muhlschlegel, H. J. Eisler, O. Martin, B. Hecht, and D. Pohl, "Resonant optical antenna," *Science*, vol. 308, pp. 1607–1608, 2005.

[4] D. Dregely, R. Taubert, J. Dormüller, R. Vogelgesang, K. Kern, and H. Giessen, "3D optical Yagi-Uda nanoantenna array," *Nature Commun*., vol. 2, pp. 1–7, art no. 267, 2011.

[5] L. Novotny, "Effective wavelength scaling for optical antennas," *Phys. Rev. Lett*., vol. 98, pp. 266802-1–266802-4, 2007.

[6] N. Engheta, A. Salandrino, and A. Alu, "Circuit elements at optical frequencies: Nanoinductors, nanocapacitors and nanoresistors," *Phys. Rev. Lett*., vol. 95, pp. 095504-1–095504-4, 2005.

[7] F. P. G. De Arquer, V. Volskiy, N. Verellen, G. A. E. Vandenbosch, and V. V. Moshchalkov, "Engineering the input impedance of optical nanodipole antennas: Materials, geometry and excitation effect," *IEEE Trans. Antennas Propag*., vol. 59, no. 9, pp. 3144–3153, Sep. 2011.

[8] J. A. Stratton, "Oscillations of a sphere," in *Electromagnetic Theory*. New York: McGraw-Hill, 1941.

[9] J. D. Jackson, "Modes in a rectangular waveguide," in *Classical Electrodynamics*, 3rd ed. New York: Wiley, 1998.

[10] C. E. Baum, "The singularity expansion method: Background and developments," *IEEE Antennas Propag. Soc. Newslett*., vol. 28, no. 4, pp. 14–23, Aug. 1986.

[11] R. F. Harrington and J. R. Mautz, "Control of radar scattering by reactive loading," *IEEE Trans. Antennas Propag*., vol. 20, no. 4, pp. 446–454, Jul. 1972.

[12] D. R. Fredkin and I. Mayergoyz, "Resonant behavior of dielectric objects (electrostatic resonances)," *Phys. Rev. Lett*., vol. 91, pp. 253902-1–253902-4, 2003.

[13] I. D. Mayergoyz, D. R. Fredkin, and Z. Zhang, "Electrostatic (plasmon) resonances in nanoparticles," *Phys. Rev. B*, vol. 72, pp. 155412-1–155412-5, 2005.

[14] J. Aizpurua, G. W. Bryant, L. J. Richter, and F. J. Garica de Abajo, "Optical properties of coupled metallic nanorods for field enhancement spectroscopy," *Phys. Rev. B*, vol. 71, pp. 235420-1–235420-13, 2005.

[15] T. J. Davis, K. C. Vernon, and D. E. Goméz, "Designing plasmonic systems using optical coupling between nanoparticles," *Phys. Rev. B*, vol. 79, pp. 155423-1–155423-10, 2009.

[16] T. J. Davis, D. E. Goméz, and K. C. Vernon, "Simple model for the hybridization of surface plasmon resonances in metallic particles," *Nano. Lett*., vol. 10, pp. 2618–2625, 2010.

[17] G. W. Milton, "Bounds on the complex dielectric constant of a composite material," *Appl. Phys. Lett*., vol. 37, pp. 300–302, 1980.

[18] G. W. Milton, "Bounds on the complex permittivity of a two-component composite material," *J. Appl. Phys*., vol. 52, pp. 5286–5293, 1981.

[19] G. W. Milton, "Bounds on the transport and optical properties of a two-component composite material," *J. Appl. Phys*., vol. 52, pp. 5294–5304, 1981.

[20] L. Sun and K. W. Yu, "Strategy for designing broadband epsilon-near-zero metamaterials," *J. Opt. Soc. Amer. B*, vol. 29, pp. 984–989, 2012.

[21] G. W. Milton, *The Theory of Composites*. Cambridge, U.K.: Cambridge Univ. Press, 2002.

[22] H. Huwata, H. Tamaru, K. Esumi, and K. Miyano, "Resonant light scattering from metal nanoparticles: Practical analysis beyond Rayleigh approximation," *Appl. Phys. Lett*., vol. 83, pp. 4625–4627, 2003.

[23] V. K. Valev, A. V. Silhanek, Y. Jeyaram, D. Denkova, B. De Clercq, V. Petkov, X. Zheng, V. Volskiy, W. Gillijns, G. A. E. Vandenbosch, O. A. Aktsipetrov, M. Ameloot, V. V. Moshchalkov, and T. Verbiest, "Hotspots decorations map plasmonic patterns with the resolution of scanning probe techniques," *Phys. Rev. Lett*., vol. 106, pp. 226803-1–226803-4, 2011.

[24] V. K. Valev, D. Denkova, X. Zheng, A. I. Kuznetsov, C. Reinhardt, B. N. Chichkov, G. Tsutsumanova, E. J. Osley, V. Petkov, B. D. Clercq, A. V. Silhanek, Y. Jeyaram, V. Volskiy, P. A. Warburton, G. A. E. Vandenbosch, S. Russev, O. A. Aktsipetrov, M. Ameloot, V. V. Moshchalkov, and T. Verbiest, "Plasmon-enhanced sub-wavelength laser ablation: Plasmonic nanojets," *Adv. Mater*., vol. 24, pp. 29–35, 2012.

[25] Y. Sonnefraud, N. Verellen, H. Sobhani, G. A. E. Vandenbosch, V. V. Moshchalkov, P. Van Dorpe, P. Norlander, and S. A. Maier, "Experimental realization of subradiant, superradiant, and Fano resonances in ring/disk plasmonic nanocavities," *ACS Nano*, vol. 4, pp. 1664–1670, 2010.

[26] N. Verellen, P. Van Dorpe, C. Huang, K. Lodewijks, G. A. E. Vandenbosch, L. Lagae, and V. V. Moshchalkov, "Plasmon line shaping using nanocross for high sensitivity LSPR sensing," *Nano. Lett*., vol. 11, pp. 391–397, 2011.

[27] R. F. Harrington, *Field Computation by Moment Methods*. New York: Wiley, 1993.

[28] G. A. E. Vandenbosch and A. R. Van Capelle, "Mixed-potential integral expression formulation of the electric field in a stratified dielectric medium—Application to the case of a probe current source," *IEEE Trans. Antennas Propag*., vol. 40, no. 7, pp. 806–817, Jul. 1992.

[29] F. J. Demuynck, G. A. E. Vandenbosch, and A. R. Van Capelle, "The expansion wave concept—I: Efficient calculation of spatial Green's functions in a stratified dielectric medium," *IEEE Trans. Antennas Propag*., vol. 46, no. 3, pp. 397–406, Mar. 1998.

[30] M. Vranken and G. A. E. Vandenbosch, "Hybrid dyadic-mixed-potential and combined spectral-space domain integral-equation analysis of quasi-3-D structures in stratified media," *IEEE Trans. Micro. Theory Tech*., vol. 51, no. 1, pp. 216–225, Jan. 2003.

[31] Y. Schols and G. A. E. Vandenbosch, "Separation of horizontal and vertical dependencies in a surface/volume integral equation approach to model quasi 3-D structures in multilayer media," *IEEE Trans. Antennas Propag*., vol. 55, no. 4, pp. 1086–1094, Apr. 2007.

[32] P. B. Johnson and R. W. Christy, "Optical constants of the noble metals," *Phys. Rev. B*., vol. 6, pp. 4370–4379, 1972.

[33] C. E. Baum, "On the singularity expansion method for the solution of electromagnetic interaction problem," *Interaction Notes*, Note 88, Dec. 1971.

[34] G. A. E. Vandenbosch, "Reactive energies, impedance, and Q factor of radiating structures," *IEEE Trans. Antennas Propag*., vol. 58, no. 4, pp. 1112–1127, Apr. 2010.

[35] S. Zhang, D. A. Genov, Y. Wang, M. Liu, and X. Zhang, "Plasmon-induced transparency in metamaterials," *Phys. Rev. Lett*., vol. 101, pp. 047401-1–047401-4, 2008.

[36] N. Verellen, Y. Sonnefraud, H. Sobhani, F. Hao, V. V. Moshchalkov, P. Van Dorpe, P. Nordlander, and S. A. Maier, "Fano resonance in individual coherent plasmonic nanocavities," *Nano Lett*., vol. 9, pp. 1663–1667, 2009.

[37] O. A. Kocharovskaya and Y. I. Khanin, "Population trapping and coherent bleaching of a three-level medium by a periodic train of ultrashort pulses," *Sov. Phys. JETP*, vol. 63, pp. 945–950, 1986.

[38] J. A. Fan, C. Wu, K. Bao, J. Bao, R. Bardhan, N. J. Halas, V. N. Manoharan, P. Nordlander, G. Shvets, and F. Capasso, "Self-assembled plasmonic nanoparticle clusters," *Science*, vol. 328, pp. 1135–1138, 2010.

Xuezhi Zheng received the B.S. degree from Tianjin Polytechnic University, Tianjin, China, in 2008, and the M.E. degree in electrical engineering from Katholieke Universiteit Leuven, Leuven, Belgium, in 2010, where he is currently working toward the Ph.D. degree.

His research interests include the computational aspects of light–matter interaction at nanoscale and the optical confinement phenomena in plasmonic nanomaterials with predesigned electromagnetic properties.

Vladimir Volskiy (M'00) received the Graduate's degree from the Moscow Power Engineering Institute, Moscow, Russia, in 1987, and the Ph.D. degree in science in 1987.

In 1987, he joined the Antennas and Propagation of Radio Waves Division, Moscow Power Engineering Institute, as a Researcher. Since January 1996, he has been a Postdoctoral Researcher in the TELEMIC Division, Department of Electrical Engineering, Katholieke Universiteit Leuven, Leuven, Belgium. His main research interests include electromagnetic theory, computational electromagnetics, and modeling and measuring of electromagnetic radiation, including bioelectromagnetics.

Ventsislav K. Valev was born in Bulgaria. He received the Graduate's degree in Cardiff, U.K., in 2002 and the Ph.D. degree from the Radboud University Nijmegen, Nijmegen, The Netherlands, in 2006, for his work on magnetization-induced second-harmonic generation at the interfaces of magnetic thin films.

He is currently a Research Associate in the Cavendish Laboratory, University of Cambridge, Cambridge, U.K. He was a Postdoctoral Fellow at the Katholieke Universiteit Leuven, Leuven, Belgium, where he extended his expertise to the optical properties of organic molecular films and plasmonic nanostructures.

Guy A. E. Vandenbosch (SM'08) received the M.S. and Ph.D. degrees in electrical engineering from the Katholieke Universiteit Leuven, Leuven, Belgium, in 1985 and 1991, respectively.

From 1991 to 1993, he was a Postdoctoral Researcher at the Katholieke Universiteit Leuven, where he became a Lecturer in 2003, and since 2005, he has been a Full Professor. He teaches and has taught courses on "electromagnetic waves," "antennas," "electromagnetic compatibility (EMC)," "electrical engineering, electronics, and electrical energy," and "digital steer and measuring techniques in physics." His work has been published in about 150 papers in international journals and has been presented in about 250 papers at international conferences. His research interests include the area of electromagnetic theory, computational electromagnetics, planar antennas and circuits, nanoelectromagnetics, electromagnetic radiation, EMC, and bioelectromagnetics.

Dr. Vandenbosch has been a member of the "Management Committees" of the consecutive European COST actions on antennas since 1993. Within the ACE Network of Excellence of the EU (during 2004–2007), he was a member of the Executive Board and coordinated the activity on the creation of a European antenna software platform. He currently leads the EuRAAP Working Group on Software and represents this group within the EuRAAP Delegate Assembly. He is the holder of a certificate of the postacademic course in electromagnetic compatibility at the Technical University Eindhoven, Eindhoven, The Netherlands. From 2001 to 2007, he was the President of the Belgian Society of Engineers in Telecommunication and Electronics. Since 2008, he has been a member of the board of the Belgian branch of the Federation of Telecommunications Engineers of the European Union. He is currently the Chairman of the IEEE Benelux Chapter on Antennas en Propagation, where was the Vice Chairman from 1999 to 2004, and Secretary from 2005 to 2009. From 2002 to 2004, he was the Secretary of the IEEE Benelux Chapter on EMC. He is currently the Secretary of the Belgian National Committee for Radio-electricity, where he is also in charge of Commission E.

Victor V. Moshchalkov was born in Russia. He received the M.Sc., Ph.D., and Habilitation degrees in physics from the Lomonosov Moscow State University, Moscow, Russia, in 1975, 1978, and 1985, respectively.

From 1978 to 1988, he was a Research Physicist, Assistant Professor, and Professor at the Lomonosov Moscow State University where in 1988, he became the Head of the Laboratory of High Temperature Superconductivity. Since 1986, he has been a Visiting Scientist or Visiting Professor at Toronto University, Canada, Technischen Universität Darmstadt, Germany, Marburg University, Germany, RWTH Aachen, Germany, and Centre d'Etudes Nucléaires de Grenoble, France. In 1991, he joined the Katholieke Universiteit (K.U.) Leuven, Leuven, Belgium, as a Visiting Professor, where he became a Full Professor in 1993. He has more than 780 publications in international peer reviewed journals and more than 9300 citations. He became the Director of the Institute for Nanoscale Physics and Chemistry (Center of Excellence at the K.U. Leuven) in 2005. He has been, or is, the Promoter of 48 Ph.D. theses (12 at the Moscow State University and 36 at the K.U. Leuven).

Dr. Moshchalkov received the Young Researcher Award in 1986, the High Education Scientific Prize in 1988, the ISI Thomson Scientific Award "Top Cited Paper in Flanders" in 2000, the Dr. A. De Leeuw-Damry-Bourlart Prize for Exact Sciences from the Flemish Fund for Scientific Research in 2005, and the Methusalem Research Award in 2009. He was a finalist for the European Union Descartes Research Prize in 2006. Since 2007, he has been an American Physical Society Fellow. From 1999 to 2004, he was the Chairman of the European Science Foundation (ESF) Program "Vortex Matter in Superconductors-VORTEX. Since 2007, he has been the Chairman of the ESF program on Nanoscience and Engineering in Superconductivity, which includes 60 teams from 15 European countries. He was an Invited Speaker at 96 international conferences and workshops, and is the Founder of the new series of International Conferences on "Vortex Matter in Nanostructured Superconductors." He is a member of the International Advisory Committee of 34 international conferences.